

# Conceptualization and Application of Unmanned Aerial Vehicles Design Methodology

Daniel Patinha Coelho  
daniel.coelho@tecnico.ulisboa.pt

*Instituto Superior Técnico, Universidade de Lisboa, Portugal*

July 2019

## Abstract

Unmanned Aerial Vehicles (UAV) are the subject of study for over half a century. The first steps taken into the world of unmanned aircraft were mostly bounded with adapting existent manned aircraft into unmanned. With the technological evolution experienced in the recent decades UAV emerged as unique aircraft with a dedicated branch of the aviation industry. Despite this fact, the UAV world is yet somewhat secret when it comes to the conceptual design of such machines. As there are methodologies for manned aircraft conceptual design, provided by authors such as Jan Roskam, Daniel P. Raymer, Thomas C. Corke and Mohammad H. Sadraey, among others, a similar methodology should also be developed for the design of fixed-wing UAV. Albeit such methodology may be partially based on the existent manned aircraft conceptual design methodologies, there are many details that impose a great difference between manned and the existent unmanned aircraft, from the usually different take-off mass to the overall configuration of the aircraft. The uniqueness of UAV in comparison with manned aircraft becomes even more evident as the Reynolds number experienced in flight decreases, due to the smaller size and lower flight speeds. The conceptualization and application of such methodology is the purpose of this work, which culminates in the development of a Medium Altitude Long Endurance (MALE) class UAV to be ultimately manufactured by UAVision Aeronautics.

**Keywords:** Conceptual Design Methodology, Unmanned Aerial Vehicle (UAV), Remotely Piloted Aerial Vehicle (RPAV), Medium Altitude Long Endurance (MALE), Low Reynolds.

## 1. Introduction

Technological advances in the aviation industry throughout the past century provided the world with two kinds of unmanned aircraft, they are the Unmanned Aerial Vehicles (UAV) and the Remotely Piloted Aerial Vehicles (RPAV), which are both commonly referred to as drones. Despite the differences, since both are unmanned, the term UAV may be considered as the generic title, although, the UAV developer and user community uses the term UAV to refer to an unmanned aircraft capable of performing autonomous and preprogrammed missions whilst the term RPAV is used to describe an unmanned aircraft piloted from a remote location.

The reality of the aviation industry in the XXI century allowed the growth of the worldwide interest in the ever-improving concept of UAV. In fact, aside the military world, UAV have been developed for a variety of civil applications, from structural inspection, topographic analysis, crops surveillance and payload delivery, to search and rescue missions.

Despite the visible growth of the UAS industry there still isn't an established methodology for the design of UAV as there are for manned aircraft, provided by numerous authors such as J. Roskam [1, 2], M. H. Sadraey [3], D. P. Raymer [4] and T. C. Corke [5], among others. The reason probably rests with the economic interest of the many entities already manufacturing and retailing UAV.

The work described in this paper was developed with the primary objective of suggesting changes to the existent conceptual design methodologies for manned aircraft, so to come up with a methodology best fitted for the conceptual design of fixed-wing UAV. A secondary objective was to develop the preliminary design of a Medium Altitude Long Endurance (MALE) class UAV with requirements provided by UAVision Aeronautics, a portuguese UAV manufacturer which cooperated in the development of this work. Such requirements include a maximum payload of 150Kg and a minimum endurance for maximum payload of 15 hours, as well as the compliance with international aviation regulations.

## 2. Methodology

Different authors propose different descriptions for the design process of an aircraft, despite they all end up reflecting more or less the same process and the same steps, only with different designations and sometimes with a different order for addressing design steps. Therefore, albeit some small differences, there is no methodology better than the others and it is up to the designer to select which of the authors to follow. In the present work the methodology followed is the one proposed by T. C. Corke [5], although the order of addressing design steps is not entirely the same.

**Table 1:** Different tail and engine configurations of the unmanned aerial vehicles considered in the database.

Tail Configuration	N
Conventional V-tail (CVT)	4
Boom Mounted V-tail (BMVT)	1
Conventional T-tail (CTT)	6
Conventional A-tail (CAT)	3
Boom Mounted A-tail (BMAT)	9
Conventional Y-tail (CYT)	1
Boom Mounted H-tail (BMHT)	9
Boom Mounted Inverted U-tail (BMIUT)	2
Boom Mounted II-tail (BMPT)	2
Boom Mounted L-tail (BMLT)	1
Engine Configuration	N
Aft Tail Mounted Engine (ATME)	7
Aft Fuselage Mounted Engine (AFME)	21
Fuselage Mounted Twin Engines (FMTE)	2
Wing Mounted Twin Engines (WMTE)	3
Wing Mounted Engine (WME)	3
Nose Mounted Engine (NME)	2

To support the present work a database of UAV was created. Despite the efforts to acquire the maximum amount of technical information regarding as many different UAV as possible, the success was not as notorious as it could be due to the fact that most of the UAV manufacturers that have been contacted were not keen to provide such information, as they find it classified. Therefore it was only possible to collect data from UAV whose manufacturers have already made technical data available to the general public. The specifications of each of these UAV, which provided the basis for the later estimations of several different design and performance parameters, were obtained either on their respective manufacturer brochure, upon direct contact with the respective manufacturer or by computation using the specific parameters available. As a way of supporting the results, the UAV selection was performed aiming to collect information on UAV with different configurations regarding the type of tail moutage and shape and also engine positioning. Table 1 shows the different configurations considered and the number of UAV, N,

on the database with such configurations.

Several technical parameters of the UAV in the database were studied and related to each other with the scope of finding relations from which to support the changes to the conceptual design values and procedures that will be proposed.

Despite the low number of UAV exemplars, the database served its purpose which was to prove by simple assumptions, supported by the relations and proposals provided by T. C. Corke and the other already mentioned authors [1, 3, 4, 5], that the values for a number of parameters used in the conceptual design of a manned aircraft do not apply for UAV conceptual design.

## 3. Unfit Methodology Details

The importance of outlining the details on the manned aircraft conceptual design methodology unfit for the design of UAV, and ultimately propose more fitted values for them, is bound with the fact that a more accurate initial guess will help reducing the number of iterations needed in the conceptual design process of an UAV. For that matter, such details are here outlined and an explanation is provided regarding the reason why they are unfitted.

The lift-to-drag ratio,  $\frac{L}{D}$ , is used in the Maximum Take-off Mass (MTOM) estimation through the computation of the fuel fractions. In the first step of the conceptual design it must be estimated as a percentage of the maximum lift-to-drag ratio,  $(\frac{L}{D})_{max}$ , which by itself is also estimated.

The Structural Factor (SF) is also used in the MTOM estimation and its purpose is to account for the empty mass of the aircraft. Provided the present technologies regarding the use of composite materials it is not unusual to encounter UAV with structural factors much lower than those of manned aircraft.

The aspect ratio, A, has a major impact on the aircraft overall efficiency and, despite being somewhat a designer choice, may be influenced by mission requirements. For example, if one UAV is to be designed aiming for efficient long endurance missions it requires an high A. On the other hand, if the mission requirements impose some sort of span limit the initial A guess must be a lower value.

The fuel consumption, C, is an engine-related parameter which will affect the MTOM estimation through the computation of the fuel mass fractions on the cruise and loiter flight phases. In the literature [1, 3, 4, 5] values are proposed for several types of engines used in manned aircraft. The problem is that propeller driven UAV use smaller engines thus reflecting other values for specific fuel consumption.

The efficiency factor, also known as Oswald's coefficient, which will be represented in this docu-

ment by  $e_f$  to avoid confusion with the exponential symbol  $e$ , has an inverse influence on the induced drag coefficient,  $C_{D_i}$ , and by extension in the overall drag coefficient of the wing of an aircraft [1]. This fact then causes a problem since the value of 0.8 proposed in the literature [5, 3] for this parameter may be very far from the values obtained for the majority of UAV.

The zero lift drag coefficient,  $C_{D_0}$ , requires an initial guess and a problem arises regarding the values proposed in the manned aircraft conceptual design methodologies [1, 3, 4, 5] because UAV present a much wider range of values for this parameter.

Despite not presenting any novelty, the airfoil, taper ratio,  $\lambda$ , and sweep angle,  $\Gamma$ , selection has a big impact on the overall efficiency of the wing and therefore on that of the UAV itself. Therefore, when it comes to the efficiency-wise wing design of an UAV it is of importance to provide some considerations.

Since on UAV there is no need to accommodate crew, the fuselage design is aimed to the accommodation of all the systems and payload. Regarding the fineness ratio of the fuselage, which is given by the ratio between the fuselage maximum diameter and its length, the goal is to demonstrate which UAV configuration promotes the best efficiency-wise fineness ratio,  $\frac{d}{l}$ .

The tails positioning, given by the  $\frac{\ell_T}{\ell_{Total}}$ , where  $\ell_T$  is the distance between the wing and the horizontal and vertical tails aerodynamic centers and  $\ell_{Total}$  is the aircraft overall length, and the horizontal and vertical tail size coefficients end up working hand-to-hand in the design of an UAV and reflect a compromise between the tails distance to the wing and their sizes, so that the aircraft is statically stable. Through the study of the UAV database developed, considerations will be presented regarding these parameters and a process for estimating an empirical value for the horizontal tail size coefficient will be provided.

#### 4. Proposed Methodology Adaptations

In this chapter a discussion is placed regarding each of the parameters that were pointed out in the previous chapter and ultimately an estimate or a proposal for the estimation of such parameters is provided. The parameters found to be troublesome were basically related to four different steps of the conceptual design methodology: the TOM estimation, the wing design, the fuselage design and the tail design. Given this situation and for organization purposes the present chapter is then divided in four sections, each dedicated to one of the aforementioned design steps.

#### 4.1. Maximum Take-off Mass Estimation

The maximum take-off mass, MTOM or  $m_{To}$ , of an UAV may be estimated by equation 1, where  $m_{pl}$  is the payload mass,  $m_e$  is the empty mass of the aircraft,  $m_{fuel}$  is the fuel mass and  $m_{res}$  is the reserve fuel mass, given as a percentage of  $m_{fuel}$ . At this stage the payload requirement is already established and thus  $m_{pl}$  is known.

$$m_{To} = m_{pl} + m_e + m_{fuel} + m_{res} \quad (1)$$

The  $m_e$  estimation is performed in the literature [1, 3, 4, 5] through the use of a Structural Factor (SF), according to equation 2. At the current stage of the UAV industry, the SF depends mostly on the efficiency (mass-wise) of the composite materials used as well as the construction methods. In the UAV studied the SF may be as low as around 0.3, nonetheless, a good initial guess for the structural factor is 0.5 because, as explained, the SF depends on materials and methods which may not be perfect.

$$m_e = SF \times m_{To} \quad (2)$$

The typical flight plan of an UAV is comprised by five different flight phases: *Engine Start-up and Take-off*, *Climb and Acceleration to Cruise*, *Cruise*, *Loiter* and *Landing*. As proposed by T. C. Corke [5], the mass of fuel needed is computed through fuel mass fractions for each mission phase, as shown by equation 3 where  $m_N$  is the aircraft mass at the  $N^{th}$  flight phase.

$$m_{fuel} = \left[ 1 - \frac{m_2}{m_1} \times (\dots) \times \frac{m_N}{m_{N-1}} \right] \times m_{To} \quad (3)$$

For the *Engine Start-up and Take-off* and *Landing* phases, the fuel mass fraction proposed is shown in equation 4, where  $m_i$  represents the aircraft mass at the beginning of one flight phase and  $m_f$  the mass at the end of that same flight phase.

$$0.97 \leq \left( \frac{m_f}{m_i} \right) \leq 0.975 \quad (4)$$

Regarding the *Climb and Acceleration to Cruise* phase, the proposal is to consider a fuel mass fraction of 0.99, for UAV flying below Mach 0.2 (as is the case for the vast majority).

Regarding the fuel mass fractions for the *Cruise* and *Loiter* phases, they are computed through equations 5 and 6, respectively, where  $R$  is the range,  $C$  is the engine specific fuel consumption,  $\eta$  is the propulsive efficiency,  $V_{Lt}$  is the loiter speed,  $E$  is the endurance and  $\frac{L}{D}$  is the lift-to-drag ratio.

$$\left( \frac{m_f}{m_i} \right)_{Cr} = e^{\left[ -\frac{RC}{\eta \left( \frac{L}{D} \right)} \right]} \quad (5)$$

$$\left(\frac{m_f}{m_i}\right)_{Lt} = e^{\left[-\frac{EV_{Lt}C}{\eta\left(\frac{L}{D}\right)}\right]} \quad (6)$$

For the fuel consumption is safe to assume in this design phase that  $C=0.5 \frac{Kg}{kWh}$  for 2-stroke engines, used normally in UAV with Maximum Take-off Mass (MTOM) below 50kg [6],  $C=0.3 \frac{Kg}{kWh}$  for 4-stroke or Wenkel engines, used in UAV with MTOM over 50kg [6]

The lift-to-drag ratio is estimated as 90% of the maximum range and maximum endurance lift-to-drag ratio,  $\left(\frac{L}{D}\right)_{R_{max}}$  and  $\left(\frac{L}{D}\right)_{E_{max}}$  (for cruise and loiter, respectively), which may be estimated with respect to the aspect ratio through equations 7 and 8, respectively, which come from the database analysis and are shown in figures 1 and 2.

As a recommendation for the aspect ratio selection, consider  $A \approx 10$  for  $E < 24h$  and  $A \approx 20$  for  $E > 24h$ .

$$\left(\frac{L}{D}\right)_{R_{max}} = 0.65A + 8.6 \quad (7)$$

$$\left(\frac{L}{D}\right)_{E_{max}} = 0.56A + 7.5 \quad (8)$$

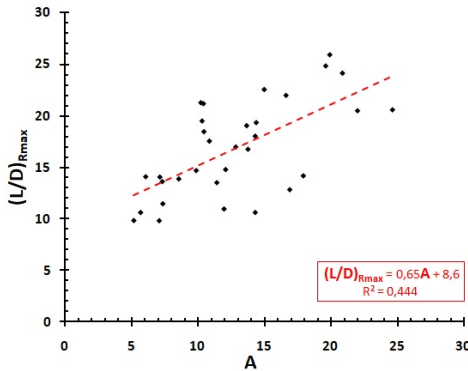


**Figure 1:** Maximum range lift-to-drag ratio against wing aspect ratio, from database.

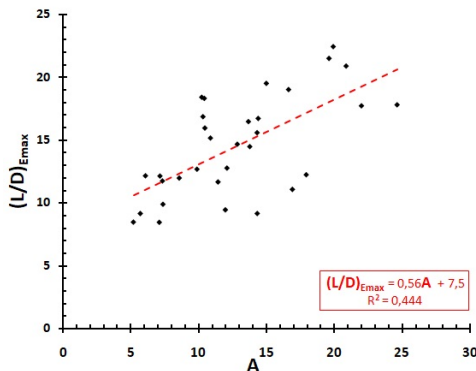


**Figure 2:** Maximum endurance lift-to-drag ratio against wing aspect ratio, from database.

## 4.2. Wing Design

There are many requirements that may influence the wing design, namely performance requirements (MTOM, cruise speed,  $V_{Cr}$ , stall speed,  $V_s$ , range, endurance, maneuverability, etc.) and structural requirements (internal volume, maximum allowed span, structural mass, etc.). In an UAV that flies at low speeds (below  $M=0.2$ ) normally the main objective in the wing design is its efficiency, whether the goal is maximum range or maximum endurance.

Regarding the airfoil selection, one of the core aspects is the thickness,  $t$ , which directly influences the choice of the airfoil through the maximum thickness-to-chord ratio,  $\left(\frac{t}{c}\right)_{max}$ . This is of utmost importance since a thinner airfoil allows for a thinner spar, which may pose a problem when designing UAV with high  $A$ . As it was proven by the United States of America National Advisory Committee for Aeronautics (NACA) [7], for a variety of airfoil sections a  $\left(\frac{t}{c}\right)_{max} \approx 14\%$  provides for the highest maximum lift coefficient ( $C_{l_{max}}$ ), thus it is a good value to aim for.

Regarding the taper ratio,  $\lambda$ , and aspect ratio,  $A$ , they both have a major influence in the overall drag coefficient,  $C_D$ , and on the efficiency of the wing by extent. In order to demonstrate the importance of a careful selection of  $\lambda$  and  $A$ , an analysis was conducted using the XFLR5 software. Several wings corresponding to increasing MTOM classes of UAV were analysed, in terms of their endurance-wise efficiency, and the results are presented in figures 3 and 4, where  $S$  is the wing planform area. The endurance of an aircraft is maximum for  $\left(\frac{C_L^3}{C_D^2}\right)_{max}$ , where  $C_L$  is the lift coefficient. In the study was considered  $\lambda=0.4$  because it is the value which best approximates and ellipse-shaped wing and from lifting line theory, an unswept, untwisted ellipse-shaped wing provides the minimum drag.

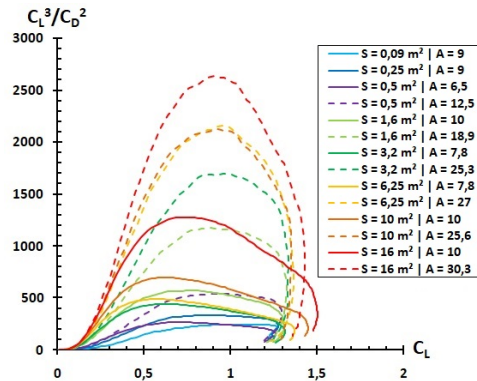


**Figure 3:** Influence of aspect ratio on the lift-to-drag ratio powered by three halves.

As for the sweep angle, the main reason for adding leading edge sweep to a wing is to delay

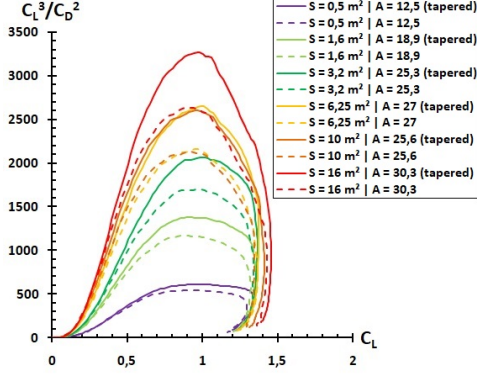


**Figure 4:** Taper ratio influence on the lift-to-drag ratio powered by three halves.

and lower the drag rise that occurs when reaching transonic flight speeds. In subsonic aircraft usually there is no wing sweep because it does not improve the aerodynamics of the wing and in fact the wing mass increases by adding sweep, according to historical data [5]. As a result, the optimum leading edge sweep for a subsonic UAV is no sweep at all.

Regarding the wing drag estimation there are two major aspects to consider, the formulation used to compute it, which has a big impact through the manner of computing the efficiency factor,  $e_f$ , and the zero lift drag coefficient,  $C_{D_0}$  considered. Three formulations were considered, proposed by T. C. Corke (equations 9), by I. Grosu (equations 10) and by B. W. McCormick (equations 11). Here  $\delta$  is a parameter that corrects the departure of the loading distribution from elliptic, as explained by G. R. Spedding and J. McArthur [8], and  $k$  is a parameter that corrects the departure from the presumed parabolic shape of the airfoil drag polar.

$$C_D = C_{D_0} + \frac{C_L^2}{\pi A e_f} \quad (9a)$$

$$e_f = \frac{1}{1 + \delta} \quad (9b)$$

$$C_D = C_{D_0} + 0.028 \left( \frac{t}{c} \right)_{max} + 1.08 \frac{C_L^2}{\pi A} \quad (10a)$$

$$e_f = \frac{1}{1.08 + \frac{0.028 (t/c)_{max} \pi A}{C_L^2}} \quad (10b)$$

$$C_D = C_{D_0} + k C_L^2 + \frac{C_L^2}{\pi A} (1 + \delta) \quad (11a)$$

$$e_f = \frac{1}{1 + \delta + k \pi A} \quad (11b)$$

In order to compare the different  $C_D$  formulations, a study was performed using XFLR5

software to obtain  $C_L$  values from three different untwisted rectangular wings corresponding to  $Re=100k$ ,  $Re=1M$  and  $Re=3M$ . Afterwards, the obtained  $C_L$  values were used to compute  $C_D$  using equations 9, 10 and 11. Figure 5 shows the results of comparison, from which it is straightforward to conclude that the formulation proposed by B. W. McCormick is the most conservative and thus its use is recommended. It is important to mention that the vertical displacement between each  $Re$  is only for visualization purposes and was achieved by providing each  $Re$  with a different value for  $C_{D_0}$ . This fact does not influence the evaluation and comparison between each  $C_D$  formulation since all of them are dependent of  $C_{D_0}$  in the same way and the comparison between them is made within each  $Re$  and therefore within the same value for  $C_{D_0}$ .

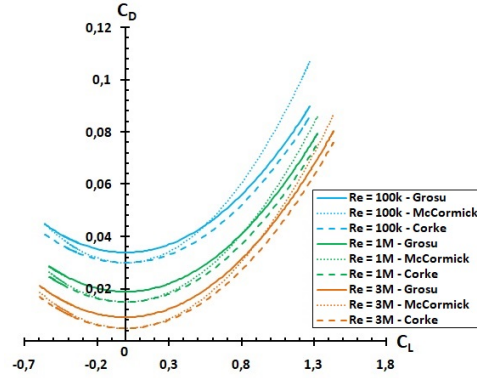


**Figure 5:** Comparison between the presented formulations for estimating the drag coefficient of an aircraft.

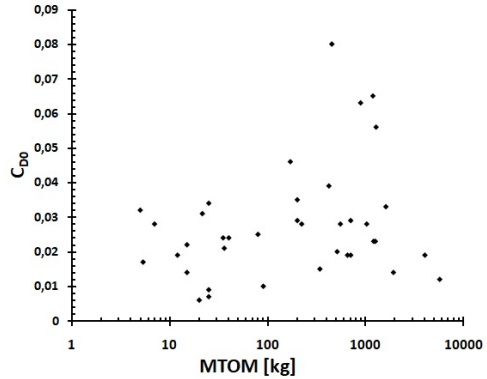


**Figure 6:** Zero lift drag coefficient distribution with the maximum take-off mass, from database.

As for  $C_{D_0}$ , figure 6 shows the study of this parameter for the UAV in the database and allow for the conclusion that for the UAV studied the range of  $C_{D_0}$  values is approximately  $0.005 \leq C_{D_0} \leq 0.08$ , which is very different from the  $0.01 \leq C_{D_0} \leq 0.02$  range proposed by T. C. Corke for manned aircraft. The proposed solution is to consider an interference factor,  $Q$ , of 3 when computing the aircraft  $C_{D_0}$  through the method proposed in the literature [1, 3, 4, 5], following equation 12, where  $C_f$  is the friction coefficient,  $\mathcal{F}$  is the form factor,  $S_{wet}$  is the

wing wetted (or surface) area and  $S$  is the wing planform area.

$$C_{D_0} = C_f \mathcal{F} Q \frac{S_{wet}}{S} \quad (12)$$

### 4.3. Fuselage Design

The fuselage design of an UAV may be performed with mainly two considerations which are the amount of space needed for accommodating system components and payload and the fuselage drag. The goal is to design a fuselage that can fit everything inside and that causes low drag, thus providing a lower overall drag coefficient,  $C_{D_{total}}$ . The fuselage drag is influenced by the fineness ratio,  $\frac{d}{\ell}$ , and so it will decrease as the fineness ratio lowers. From the literature [5, 3], the fineness ratio which minimizes drag is 0.3.

The fineness ratio was computed for the UAV in the database using the fuselage length,  $\ell_{fus}$ , and the equivalent maximum diameter,  $d_{max}$ , and it is shown in figure 7, where it is possible to observe that for UAV with a boom mounted tail (BMT) the fineness ratio is closer to the optimum ( $\frac{d}{\ell} \approx 0.3$ ) than for UAV with fuselage mounted tail (FMT) configuration. This has a logical explanation since for two aircraft with the same overall length,  $\ell_{Total}$ , and same  $d_{max}$ , one with BMT and the other with FMT, the fuselage length is larger in the second aircraft. As a consequence  $\frac{d}{\ell}$  will be lower on the FMT aircraft than on the BMT aircraft.

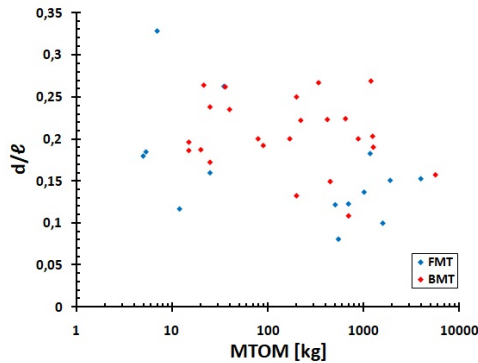


**Figure 7:** Fineness ratio against maximum take-off mass, differing by tail mount configuration, from database.

### 4.4. Tail Design

The tail conceptual design rests basically upon estimating the position of the horizontal and vertical tails, in respect to the main wing aerodynamic center, and their respective areas,  $S_{HT}$  and  $S_{VT}$ . This is performed based on wing data such as the span,  $b$ , the mean aerodynamic chord,  $\bar{c}$ , and the area, here represented by  $S_W$  to avoid confusion.

In order to understand if the values proposed in the literature [5, 3] for the horizontal and vertical tail size coefficients,  $C_{HT}$  and  $C_{VT}$ , and the length

ratio,  $\frac{\ell_T}{\ell_{Total}}$ , apply to the conceptual design of UAV, the necessity came to determining these properties for the UAV presented in the database. This properties were also studied with respect to the tail configuration and the engine(s) positioning.

Regarding the length ratio, figure 8 shows its distribution with the MTOM for the UAV in the database and table 2 shows the proposed ranges to be applied in UAV design, regarding the engine positioning (see table 1).

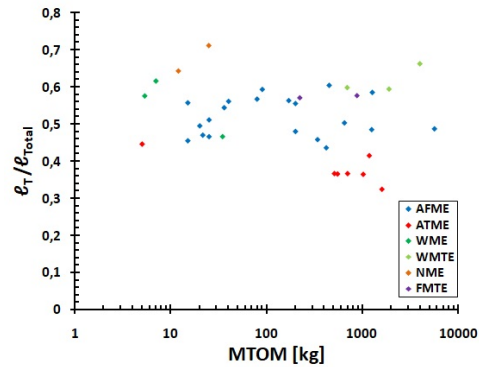


**Figure 8:** Length ratio for different engine positioning configurations.

**Table 2:** Length ratio range proposed for unmanned aerial vehicles regarding different engine position arrangements.

Engine configuration	$\ell_T/\ell_{Total}$
AFME	0.3 - 0.45
ATME	0.4 - 0.6
FMTE	0.55 - 0.6
WME or WMTE	0.55 - 0.65
NME	0.6 - 0.7

Regarding  $C_{HT}$ , its range was found to be approximately  $0.1 \leq C_{HT} \leq 1.3$  for the UAV in the database. Also, the most relevant relation found was with the aspect ratio,  $A$ , and the engine positioning, as shown in figure 9. Based on the analysis performed to this parameter, the ranges proposed for its value are shown in table 3.

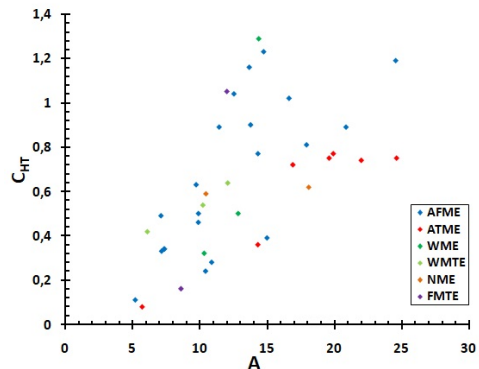


**Figure 9:** Horizontal tail size coefficient versus wing aspect ratio for different engine positioning configurations, from database.

Furthermore, an approach was developed to estimate  $C_{HT}$  based on empirical data from the

**Table 3:** Horizontal tail size coefficient range proposed for different engine position configurations.

Engine Position	$C_{HT}$
WME	0.3 - 0.65
NME	0.6
ATME ( $A < 16$ )	0.3 - 0.6
ATME ( $A \geq 16$ )	0.6 - 0.8
AFME ( $A < 11$ )	0.1 - 0.65
AFME ( $A \geq 11$ )	0.75 - 1.2

database. With the wing A find the  $\frac{\ell_{Total}}{b}$  ratio through equation 13. Then, multiply the obtained  $\frac{\ell_{Total}}{b}$  ratio by the wing span, b, to obtain the aircraft total length,  $\ell_{Total}$ . From table 2 choose the  $\frac{\ell_T}{\ell_{Total}}$  ratio that best fits the configuration of the UAV in project. Multiply the chosen  $\frac{\ell_T}{\ell_{Total}}$  ratio by  $\ell_{Total}$  to obtain  $\ell_T$ . Then, knowing the wing mean aerodynamic chord,  $\bar{c}$ , compute the ratio  $\frac{\ell_T}{\bar{c}}$  and with the computed  $\frac{\ell_T}{\bar{c}}$  ratio find  $C_{HT}$  for the UAV in project through equation 14.

$$\frac{\ell_{Total}}{b} = -0.015A + 0.8 \quad (13)$$

$$C_{HT} = 0.2 \frac{\ell_T}{\bar{c}} - 0.15 \quad (14)$$

Regarding  $C_{VT}$ , its distribution with the MTOM is presented in figure 10. It is of importance to mention that different relations were tested with the goal of finding a better way for estimating  $C_{VT}$ , nonetheless neither of the attempts revealed a clear relation. Albeit, the vertical tail size coefficient is not that important for the overall conceptual design of an aircraft, therefore the suggestion is to use  $C_{VT}=0.035$  as a first estimate when doing the conceptual design of an UAV, which corresponds to the average  $C_{VT}$  on the UAV studied.

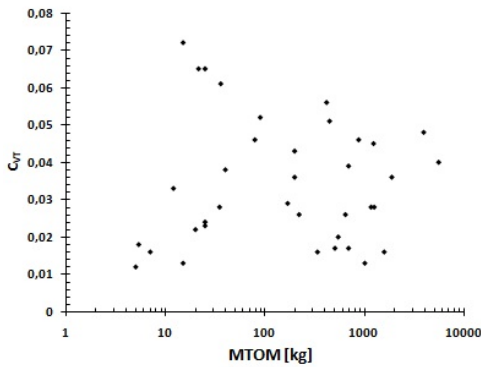


**Figure 10:** Vertical tail size coefficient distribution with MTOM, from database.

#### 4.5. Verification of the Proposed Adaptations

In order to verify the proposed adaptations to the conceptual design methodology, three UAV were selected from the database and the conceptual design proceedings were applied, along with the proposals made. The goal was to prove

that by following these proposals, based on performance requirements, the resulting aircraft would be very similar, thus verifying the adapted methodology. The UAV were selected from different mass classes so to prove the viability of the presented solutions. The chosen exemplars were the Predator, manufactured by General Atomics, the Hermes 450, manufactured by Elbeit Systems, and the Ogassa, manufactured by UAVision Aeronautics.

Since the same set of requirements can lead to entirely different aircraft configurations, depending on the designers choices, the span of each UAV was chosen to be the same as the value on the database, simply because to validate the methodology it was necessary to select either the span or the aspect ratio to remain equal to the database value, otherwise the resulting aircraft could be entirely different.

To better visualize the magnitude of the differences between the database values and the computed ones, the relative error was obtained for each property, other than b, and is shown in percentage in figure 11.

In the first three parameters,  $S_W$ , A and P, the result observable in figure 11 showing the higher errors associated to Ogassa, the intermediate to Hermes 450 and the lower to Predator, is to be expected. The reason for this fact is justified by the difference of mass class between the three UAV, since higher MTOM values usually imply bigger wing areas, higher aspect ratios and more powerful propulsion systems.

As for the two last parameters,  $S_{HT}$  and  $S_{VT}$ , figure 11 shows the highest relative error at about 6% for both, nonetheless, by inspection the values involved this errors become insignificant. For the  $S_{HT}$  the highest error is of about 6.3% for Predator's horizontal tail, which represents a difference of  $0.123m^2$  in a real area of almost  $2m^2$ . As for the  $S_{VT}$ , the highest error is of about 6.2% for the vertical tail of Hermes 450, representing a difference of only  $0.044m^2$  in a real area of nearly  $0.7m^2$ .

The highest relative error presented in figure 11 is 7.43% and it is related to the tail positioning of Hermes 450, through  $\ell_T$ . The database  $\ell_T$  value for this aircraft is 2.234m while the computed value is 2.4m, meaning that the difference between them represents less than 0.2m. A difference of 0.2m in an aircraft with a real overall length of 6.1m would represent a forward displacement of the wing of about 3.28%, which would be almost imperceptible on a first glance and would also be neglectable performance-wise.

Furthermore, the methodology proposed is to be used for the conceptual design of UAV and the results obtained in a conceptual design phase may not be the same as in a later detailed design phase.

With this in mind, an error of 7.43% is acceptable. Also, as previously explained, the conceptual design phase suits the purpose for a not that detailed first design of an aircraft, therefore the proposed methodology and adaptations may well be used. Having all this in consideration it becomes clear that the proposed adaptations to the methodology do apply to the conceptual design of unmanned aerial vehicles, and are thus validated.

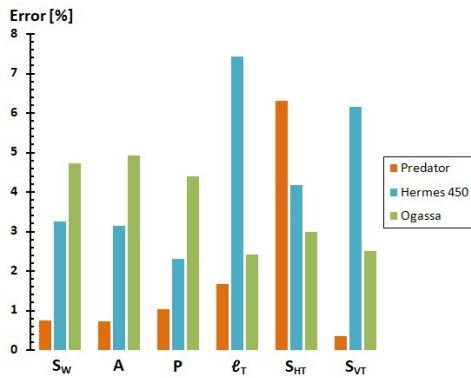


**Figure 11:** Relative error of each computed property for the selected aircraft.

## 5. MALE UAV Design Project

After the conceptualization and verification of a methodology fitted for the conceptual design of UAV, it was time to develop the conceptual design of new UAV. Driven by UAVision longing to develop an UAV for the  $150\text{kg} < \text{MTOM} \leq 600\text{kg}$  class, the requirements were set and the methodology applied. The aircraft was baptized as Heimdall, after the ever-vigilant guardian of the gods stronghold, Asgard, from Norse mythology, and it is a Medium Altitude Long Endurance (MALE) class UAV. The mission goals for Heimdall are those commonly seen in typical surveillance missions. The aircraft must be able to sustain flight for a considerable amount of time, acquire graphical data from the surveillance targets and perform target acquisition and locking, among other things. Also, the aircraft must be equipped with a radar and a satellite communication system. Furthermore, the Heimdall project is to be developed in accordance with international aviation regulations, thus complying with European Aviation Safety Agency (EASA) regulations [9], Federal Aviation Administration (FAA) regulations [10], as well as with North Atlantic Treaty Organization (NATO) regulations [11].

The following list reflects the specific requirements for the MALE UAV developed in this work, which were provided by UAVision.

- Maximum take-off mass - 600kg
- Maximum payload - 150kg
- Fuel reserve at landing - 5%

- Minimum endurance for maximum payload - 15h
- Cruise and loiter ceilings - 22000ft
- Stall speed - 25m/s
- Cruise speed - 50m/s
- Loiter speed - 40m/s
- Dash speed - 65m/s
- Min. climb speed from mean sea level - 5m/s
- Max. take-off distance - 1000m
- Min. performance load factor - -1.5
- Max. performance load factor - 2.5
- Limit load factors to be sustained by the structure in flight -  $-1.52 \leq n \leq 3.8$  [11]
- Structural safety factor - 1.5 [11]
- Min. sustainable gusts at cruise - 15m/s [11]
- Min. sustainable gusts at dash - 7.6m/s [11]
- Min. bank allowed for take-off and landing -  $5^\circ$

Regarding the surveillance, communication and sensing requirements, to be matched by payload equipments (gimbal camera, satellite communication system and radar system), a market study was performed by UAVision communications and imagery specialists to select the equipments best fitted for the application. The selected gimbal camera was the L3 MX-15D and also other two cameras were considered, the L3 MX-10D and the Octopus Epsilon 175. The radar solution considered was the Garmin 18xHD radar dome, for being lightweight and capable of matching the needed radar accuracy. Finally, the equipment selected to enable satellite communications was a specially light system developed by Ultisat.

As above mentioned, the methodology and adaptations proposed for the conceptual design of UAV were followed. In the regards of this document only the relevant aspects of the design are presented.

The design point selection, which reflects the selection of the wing loading,  $\frac{W}{S}$ , and power loading,  $\frac{W}{P}$ , is influenced by the requirements. After analysis, the selected design point was  $\frac{W}{S} = 400 \frac{N}{m^2}$  and  $\frac{W}{P} = 0.078 \frac{N}{W}$ .

Regarding the wing and enhanced lift devices design, table 4 shows the selected wing planform shape, where  $b$  is the span,  $c_{root}$  is the root chord and  $c_{tip}$  is the tip chord. The selected airfoil was the NACA 5415, and, regarding the enhanced lift devices, trailing edge plain flaps were considered and the resulting computed maximum lift coefficient of the aircraft (with flaps down) is 2.477.

Regarding the tail design, table 5 presents some properties of the selected tail configuration.

As for the engine selection, a search was conducted among some of the renown UAV engine manufacturers to find suitable engine candidates. The final decision was to use two RT600LCR-EXE engines manufactured by Rotron which provide a combined maximum continuous power output of 79kW.

**Table 4:** Heimdall wing planform shape parameters.

Parameter	Value
S	14.7m <sup>2</sup>
b	20m
A	27.21
$\lambda$	0.4
$c_{root}$	0.91729m
$c_{tip}$	0.36692m
$\bar{c}$	0.77970m

**Table 5:** Heimdall's tail shape parameters.

Parameter	Value
$\ell_T$	3.996m
S	5.11m <sup>2</sup>
Half span (b/2)	3.573m
A	10
$\lambda$	0.4
$c_{root}$	1.02m
$c_{tip}$	0.408m
V angle	89.44°

As for the fuselage design, its main purpose is the definition of the placement of each component. Since the position of the components directly influences the aircraft CG, and therefore its stability, this design step was performed by iterating with the refined mass and static stability analysis. Regardless of the fact that a FMT provides less overall efficiency than a BMT, the aircraft was designed with a FMT configuration by choice of UAVision. Also, albeit not required, the liberty was taken to establish a component layout which would allow for the setting of not one but three cargo bays.

The structure design and material selection is a design step of utmost importance when it comes to the aircraft performance. The aircraft structure must be designed to sustain the loads that may be experienced during operation as well as those imposed by international regulations. All this keeping in mind the objective of developing the aircraft with an empty mass as low as possible. It is usual in this design step to compute the aircraft V-n diagram showing the aircraft flight envelope. For that purpose, table 6 shows some of the parameters used upon computing the V-n diagram, where  $\hat{u}$  is the average gust normal speed component.

The decision for Heimdall's project was to have the entire structure made of composite materials only using an aluminum alloy where fittings and mounts would exist, simply because fiber compos-

**Table 6:** Parameters used for computing Heimdall's V-n diagram.

Parameter	Value
Performance load factor range	-1.5 ≤ n ≤ 2.5
Design load factor range	-1.52 ≤ n ≤ 3.8
Ceiling	22000ft
$\rho$	0.6095kg/m <sup>3</sup>
g	9.786m/s <sup>2</sup>
$\hat{u}$ in loiter	12.5m/s
$\hat{u}$ in cruise	11m/s
$\hat{u}$ in high $\alpha$ flight	15m/s
$\hat{u}$ in dive	5m/s

ites are not so good when it comes to secure parts through the use of bolts and/or screws and therefore a metal surface is normally required, at least on main structural components.

The refined mass analysis is used, combining with the fuselage design, to determine the aircraft CG and its inertia. To perform this task, the positioning, dimensioning and mass estimation of each of Heimdall's components was determined and the principles proposed by P. F. Beer and R. E. Johnston Jr. [12] were applied.

Regarding the static stability analysis, it was performed using an algorithm previously developed by UAVision, which is based on the principles proposed by B. Etkin [13]. The main objective of this analysis was to compute the range of the static margin,  $k_n$ , which represents the difference between the neutral point position and the CG position, with respect to the wing aerodynamic center. The range for  $k_n$  computed in this analysis, given as a percentage of the mean aerodynamic wing chord,  $\bar{c}$ , was  $0.0827 \leq k_n \leq 1.0425$ .

Designed to perform any kind of surveillance mission and to be a versatile asset for any civil and/or military operator, Heimdall makes use of an high aspect ratio wing, to provide the needed lift with low drag, and two powerful propeller pusher engines, in order to be able to sustain flight with low fuel consumption and, at the same time, be able to achieve a respectful dash speed. Having two independent engines allows for the assurance of mission accomplishment since Heimdall can sustain cruise and loiter with only one engine operational. Moreover, table 7 presents a sum-up of Heimdall's design and performance characteristics, where Min. E is the maximum endurance for the maximum payload configuration, which reflects the minimum max. E of the aircraft, and Max. pl is the maximum payload.

## 6. Conclusion and Future Work

For the successful development of a conceptual design methodology for unmanned aircraft it would be necessary to convince all the manufacturers, or at least a large amount of them, to provide to the

**Table 7:** Heimdall design and performance parameters.

Property	Value	Property	Value
MTOM	600 kg	$\ell_{Total}$	10.5m
Max. pl	150kg	b	20m
$V_S$	25m/s	$S_W$	14.7m <sup>2</sup>
$V_{Lt}$	40m/s	$\bar{c}$	0.755m
$V_{Cr}$	50m/s	A	27.21
$V_D$	65m/s	$S_{HT}$	2.531m <sup>2</sup>
P	79kW	$S_{VT}$	2.575m <sup>2</sup>
Max. E	53.5h	$C_{D_0}$	0.0223
Min. E	19.5h		

general public data from their UAV which is now considered sensitive information, since the conceptual design of an aircraft has to be performed sometimes on empirical data. Albeit many of the data gathered in the database had to be estimated based on other properties of the aircraft and conservative assumptions, the work was not jeopardized because the goal was ultimately to prove that certain assumptions considered in the literature [1, 2, 3, 4, 5] for manned aircraft do not apply to most UAV, only being possibly fitted for UAV with the size and performance similar to a manned aircraft. This goal was duly accomplished and, as a result, the methodology to be followed in the conceptual design of an UAV may be that presented by T. C. Corke [5] or M. H. Sadraey [3], for example, applying the changes here proposed. In this regard, the major proposal regarding future work, in terms of the UAV conceptual design methodology would be to add more and more UAV to the database and ultimately obtain their data directly from the manufacturers or operators.

As for the application of the conceptualized methodology, materialized in the conceptual and preliminary design of Heimdall, it may be considered as a success. The majority of decisions regarding Heimdall's design were performed scoping to the highest overall efficiency, which translates into the highest maximum endurance. On top of that, Heimdall's fuselage layout allows the transport of extra payload inside one of its three cargo bays. Heimdall's expected performance and design characteristics are very desirable for its expected applications and UAVision it-self is very pleased with the aircraft and intends to continue its project and ultimately pass it on to production. The work that needs to be developed so forth in the Heimdall project is mainly bounded with the detailed design phase.

## References

- [1] Jan Roskam. *Airplane Design*, volume I. Roskam Aviation and Engineering Corporation, 1<sup>st</sup> edition, 1985.
- [2] Jan Roskam and Chuan-Tau Edward Lan. *Air-*

*plane Aerodynamics and Performance*. Design, Analysis and Research Corporation (DARcorporation), 1<sup>st</sup> edition, 1997.

- [3] Mohammad H. Sadraey. *Aircraft Design: A Systems Engineering Approach*. John Wiley Sons, Ltd., 1<sup>st</sup> edition, 2013.
- [4] Daniel P. Raymer. *Aircraft Design: A Conceptual Approach*. American Institute of Aeronautics and Astronautics (AIAA), Inc., 2<sup>nd</sup> edition, 1992.
- [5] Thomas C. Corke. *Design of Aircraft*. Prentice Hall, 1<sup>st</sup> edition, 2003.
- [6] M. Adamsky. Analysis of propulsion systems of unmanned aerial vehicles. *Journal of Marine Engineering Technology*, 16(4):291–297, 2017.
- [7] Ira H. Abbott, Albert E. Von Doenhoff, and Louis S. Stivers Jr. Summary of airfoil data. Technical Report 824, National Advisory Committee for Aeronautics, Langley Memorial Aeronautical Laboratory, Langley Field, Virginia., 1945.
- [8] G. R. Spedding and J. McArthur. Span efficiencies of wings at low reynolds numbers. *Journal of Aircraft*, 47(1):120–128, 2010.
- [9] *Regulation 2018/1139 of the european parliament and of the council*, chapter Annex IX - Essential requirements for unmanned aircraft. Official Journal of the European Union, July 2018.
- [10] Federal Aviation Administration. Part 23 – small airplane certification process study, July 2009.
- [11] *UAV Systems Airworthiness Requirements for North Atlantic Treaty Organization Military UAV Systems - STANAG 4671*. NATO, 1<sup>st</sup> edition, March 2007.
- [12] Ferdinand P. Beer, E. Russell Johnston Jr., David F. Mazurek, Phillip J. Cornwell, and Elliot R. Eisenberg. *Vector Mechanics For Engineers*. McGraw-Hill, 9<sup>th</sup> edition, 2010.
- [13] B. Etkin. *Dynamics of Flight*, volume I. John Wiley Sons Ltd, 3<sup>rd</sup> edition, 1982.